

Selenium Promotes Sunflower Resistance to *Sclerotinia sclerotiorum* by Regulating Redox Homeostasis and Hormonal Signaling Pathways

Zhiying Chen

China Agricultural University

Huiying Sun

Shenyang Agricultural University

Ting Hu

China Agricultural University

Zehao Wang

Shenyang Agricultural University

Wenliang Wu

China Agricultural University

Yue Liang

Shenyang Agricultural University

Yanbin Guo (✉ guoyb@cau.edu.cn)

China Agricultural University <https://orcid.org/0000-0003-0134-2849>

Research Article

Keywords: selenium, redox homeostasis, hormonal signaling pathway, necrotrophic

Posted Date: May 27th, 2021

DOI: <https://doi.org/10.21203/rs.3.rs-520544/v1>

License:   This work is licensed under a Creative Commons Attribution 4.0 International License.

[Read Full License](#)

Abstract

Sclerotinia wilt of sunflower caused by *Sclerotinia sclerotiorum* is a devastating disease causing serious loss. Selenium (Se) has a benefit effect to plant in stress tolerance. In this study, sunflower leaves treated by foliar application of Se were inoculated with *S. sclerotiorum*. Pathogenesis on the inoculated leaves and transcript levels of plant genes involved in redox homeostasis and hormonal signaling pathways were examined. Se could be detected after the foliar application and was mainly transformed to selenomethionine in sunflower. Consequently, Se pretreatment delayed the necrosis development caused by *S. sclerotiorum* and alleviated the adverse effects derived from pathogen infection by differentially balancing the regulation of enzymes involved in the redox homeostasis. Specially, the *cat* expression increased to alleviate its downregulation responded to pathogen infection at the earlier infection stage (12 hour post inoculation, hpi) while the *pod*, *gpx*, *apx*, and *nox* expressions decreased to alleviate their responsive upregulation at the later infection stages (24 and 36 hpi). Se pretreatment enhanced the regulation of genes involved in hormonal signaling pathways, in which the *AOC* and *PAL* expressions increased to enhance its upregulation induced by pathogen infection for improving resistant responses at the earlier infection stage (12 hpi), as well as the *AOC* and *PDF* expressions increased at the later infection stages (24 hpi). Besides, the *EIN2* expression increased to alleviate its downregulation at all of infection stages. Our results suggested that Se plays the beneficial effect on the resistant responses to *S. sclerotiorum* infection. This study provided a clue to improve the sustainable management of Sclerotinia wilt on sunflower by Se foliar application.

1 Introduction

Sunflower (*Helianthus annuus* L.) is an annual herbal species of the Asteraceae family with medicinal and nutritional values (Guo et al. 2017). Sunflower can be used as oilseed, snack, salad garnish, livestock and pet feed, and as ornamental plants in domestic gardens (Alagawany et al. 2015; Guo et al. 2017; Toscano et al. 2017). The global yield of sunflower is approximately 56 million tons in 2019, which makes it the second largest oil crops on harvested area (FAOSAT 2020). Sunflower is threatened by many plant diseases such as downy mildew, black stem, Phomopsis stem canker and Sclerotinia wilt (Debaeke et al. 2014). Particularly, Sclerotinia wilt caused by the fungal pathogen *Sclerotinia sclerotiorum* is considered as a devastating disease that significantly affects the quality and the yield of sunflower production (Liu et al. 2017; Seiler et al. 2017). This fungus generally causes rot damage on root, stem, and head of sunflower (Ekins et al. 2011; Seiler et al. 2017).

Plants establish complex defense mechanisms against pathogen infections, which are predominately dependent on the crosstalk regulation of reactive oxygen species (ROS) and plant hormone signaling pathways (Fujita et al. 2006). ROS generated in plant not only contributes in the regulation of plant growth and development, but also facilitates responses to environmental stresses (Suzuki et al. 2011). However, the excessive accumulation of ROS has a distressing effect on the plant and ultimately leads to cell death (Sharma et al. 2019). Therefore, plants have evolved redox homeostasis, which involves

Loading [MathJax]/jax/output/CommonHTML/fonts/TeX/fontdata.js catalase (CAT), peroxidase (POD), ascorbate

peroxidase (APX), glutathione peroxidase (GPx), and NADPH oxidase (NOX) (Tiwari et al. 2017). SOD, CAT, POD, APX, and GPx are activated to scavenge ROS while NOX is involved in generating ROS (Sharma et al. 2019). Additionally, plant defense responses appropriately depend on the coordinated regulation between ROS and plant hormone signaling pathways in environmental abiotic stresses and pathogen infection (Fujita et al. 2006; Xia et al. 2015). Plants activate the appropriate plant hormone signaling pathways including salicylic acid (SA), jasmonic acid (JA), and ethylene (ET) according to the pathogen infection (Bari and Jones 2009; Spoel and Dong 2008).

The fungus *S. sclerotiorum* is a necrotrophic pathogen with a broad host range (Bolton et al. 2006). The infection process of *S. sclerotiorum* was proposed to have two phases, in both phases this fungus can overcome plant defense response (Kim et al. 2008; Liang et al. 2018). *Sclerotinia sclerotiorum* suppresses plant ROS generation by interfering the host redox homeostasis in the first phase and promotes plant ROS production to elicit the programmed cell death in the second phase (Williams et al. 2011). For example, the activities of POD, SOD, and NOX were differentially regulated while CAT activity showed unchanged during the infection course of *S. sclerotiorum* in oilseed rape (Liang et al. 2009). The activities of APX and GPx were also regulated in common bean and tobacco challenged by *S. sclerotiorum* (Fagundes-Nacarath et al. 2018; Ma et al. 2018). Therefore, ROS modulation of host plants plays critical roles in plant defense responses to *S. sclerotiorum* infection (Ranjan et al. 2018). Plant hormone signaling pathways were also modulated in plant defense responses to *S. sclerotiorum* invasion (Guo and Stotz 2007). For example, the signaling pathways of JA and ET were involved in defense against *S. sclerotiorum* in oilseed rape (Liang et al. 2009; Zhao et al. 2009). The genes involved in the JA and ET signaling pathways were differentially expressed in the pathosystem of *S. sclerotiorum* and oilseed rape (Liang et al. 2009). Additionally, the SA signaling pathway was possibly coordinated by JA regulation at the later stage of *S. sclerotiorum* infection in oilseed rape (Nováková et al. 2014).

Management of plant diseases can be improved by manipulating macro- and micro-nutrients such as sulphur, iron, copper, and selenium (Boyd 2007; Fagundes-Nacarath et al. 2018). Selenium (Se) can improve plant resistance to abiotic and biotic stresses by regulating ROS production and plant hormone signaling pathways (El-Ramady et al. 2014). For example, Se was used to protect Indian mustard from root infection by *Fusarium* species and tomato fruits from *B. cinerea*, respectively (Hanson et al. 2003; Wu et al. 2016). Se foliar application is a safer method of Se-biofortification than Se-fertilization in soil since Se uptake is affected by soil features (Bañuelos et al. 2017; Kápolna et al. 2009; Winkel et al. 2015). However, influence of Se foliar application on sunflower infected by *S. sclerotiorum* has never been reported. In this study, the effects of Se foliar application on necrotic development of sunflowers infected by *S. sclerotiorum* were assessed and the regulation of redox homeostasis and plant hormone signaling pathways was investigated. This study provides new insights into foliar Se application for improving the sustainable management of sunflower or other plants damaged by *S. sclerotiorum*.

2 Materials And Methods

The pathogen *S. sclerotiorum* was maintained on potato dextrose agar (PDA; 200 g of potatoes, 20 g of glucose, and 18 g of agar per liter) plates in this study. The fungal strain was supplied from College of Plant Protection, Shenyang Agricultural University. Seedlings of the sunflower cultivar KWS204 (Beijing Tiankui Leader Seed Technology, Beijing, China) were grown in potting soil in a growth chamber with a photoperiod of 16-h light and 8-h dark at 22°C. Plants at the six-leaf stage (approximately four-week-old) was used for subsequent assays.

2.2 Foliar Se treatment

Sunflower leaves were sprayed with a selenite solution [i.e., sodium selenite (Sigma-Aldrich, St. Louis, MO, USA) dissolved in distilled water] at serial concentrations (20, 40, and 60 μM) with approximately 2 mL per plant until runoff. Sterile water spray was served as the control. After three days of incubation in a growth chamber, the Se-treated sunflowers were thoroughly rinsed three times with sterilized water to remove the residual selenite (Farooq et al. 2019). Thereafter, each of the six leaves of each plant was inoculated with a 3-mm diameter mycelial plug excised from the active colony edge of a *S. sclerotiorum* culture. After inoculation, all the plants were maintained in a growth chamber with 90% relative humidity. Lesions developed on the inoculated leaves were assessed at 24 hour post inoculation (hpi) by following Liang et al. (2018). The measurement was performed with ten pretreated plants and the inoculation was independently repeated three times (i.e., 60 leaves for each time), and all pretreated leaves were inoculated for each plant.

2.3 Inoculation assays

Based on the inhibitory effects and lesion differentiation under Se pretreatment and pathogen challenge, the optimal concentration of Se pretreatment was determined. Thereafter, four treatments were applied in this study: (i) pathogen inoculation after Se treatment (Seln), (ii) mock inoculation with PDA plugs after Se treatment (SeUn), (iii) pathogen inoculation after mock treatment with water (In), and (iv) mock inoculation with PDA plugs after mock treatment with water (Un). To elucidate the development of necrosis caused by *S. sclerotiorum* under the optimal Se treatment, disease severity was investigated at 12, 18, 24, 36, and 48 hpi, respectively. The leaves were photographed under a visible and high intensity UV lamp (Analytik Jena US, Upland, CA, USA) and lesion area was measured (Li et al. 2019). Furthermore, a logistic equation was constructed to differentiate necrosis development within the infection course under Seln and In treatments using the OriginPro software (version 9.1; OriginLab, Northampton, MA, USA) as described in Wang et al. (2009). For each of the time points, four plants each with six leaves (24 leaves) were randomly selected as one repeat and the inoculation assessment was independently performed three times in this analysis.

2.4 Se transformation and speciation in pretreated leaves

Total Se content in leaves was assessed using hydride generation flame atomic fluorescence spectrometry (HG-AFS; AFS-920, Beijing Jitian Instruments, Beijing, China) with three biological replicates and three technical replicates for each biological replicate (Hu et al. 2018). Briefly, 1 g of SeUn or Un leaves were cut into small pieces (150 μm), and then subjected to microwave assisted acid digestion. After

cooling down, 2.5 mL 6 M HCl was added to each sample, and then the solution was heated to 100°C for 1 hour. The obtained solution was diluted with deionized water to a final volume of 50 mL while 2 mL of the solution was injected into the HG-AFS system for Se analysis. Each sample was prepared with three replicates and analyzed for linear estimation of Se pretreatment based on regression analysis using Microsoft Excel. The linear regression of Se content and fluorescence values was built using the standard substance of sodium selenite. Blanks and a certified reference material (Chinese cabbage material, GBW 10014) were included in each batch of samples for quality control.

Additionally, Se speciation in leaves was distinguished by high-performance liquid chromatography coupled to hydride generation atomic fluorescence spectrometry (HPLC-AFS; SA-20, Beijing Jitian Instruments, Beijing, China) with three biological replicates (Wang et al. 2020). Briefly, 0.8 g of fresh leaves of SeUn or Un was hydrolyzed by 5 mL of 8 mg mL⁻¹ protease XIV (Sigma-Aldrich, St. Louis, MO, USA) at 37°C for 12 hours. The samples were centrifuged at 12000 ×g for 5 min, and the supernatant was filtered through a 0.22-µm mixed cellulose nitrate filter. The filtered samples (300 µL) were injected into HPLC-AFS system for analysis, while the total Se content of samples was detected by HG-AFS system. The Se speciation was separated using an anion-exchange column (PRP-X100, Hamilton, Switzerland), and then eluted with 40 mM (NH₄)₂HPO₄ (pH 6.0) at a flow rate of 1 mL min⁻¹. Peaks were identified according to the retention times of standard compounds [i.e., selenocystine (SeCys₂), Se-methyl-selenocysteine (MeSeCys), selenite, selenomethionine (SeMet), and selenate] purchased from the National Research Center for Certified Reference Materials, Beijing, China. The identified Se species were quantified based on the peak areas of the calibration curves using an HPLC workstation. The proportion of Se speciation in pretreated sunflower leaves was calculated using the expression: Se speciation content / total Se content of leaves × 100%. Extraction efficiency rate was calculated using the expression: total Se content of enzymatic extract / total Se content of leaves × 100%.

2.5 Effects of transformed Se on fungal growth

To further estimate the potential inhibitory effects of Se on *S. sclerotiorum* growth, the mycelial growth was assessed on PDA plates supplied with 226.1 µg L⁻¹ (Se concentration) selenite or SeMet (dissolved in distilled water) (Sigma-Aldrich, St. Louis, MO, USA), the maximal concentration that could be detected in Se-pretreated sunflower leaves. PDA plate without Se served as the control. Mycelium growth on PDA with and without Se supplement was measured at 24 and 36 hpi, which was used to differentiate mycelium growth affected by Se content in the pretreated leaves.

2.6 Expression regulation analysis

To evaluate the gene expression regulation of Se-pretreated sunflower after *S. sclerotiorum* infection, certain crucial genes (*sod*, *gpx*, *cat*, *apx*, *pod*, and *nox*) were selected to measure the regulation of redox homeostasis. The expression regulation analysis of the key genes involved in JA (*AOC* and *PDF*), ET (*EIN2*) and SA (*PAL*) pathways were also conducted for the regulation of hormonal signaling pathways. Briefly, total RNA was extracted using an Eastep Super Total RNA Extraction Kit (Promega, Madison, WI,

Loading [MathJax]/jax/output/CommonHTML/fonts/TeX/fontdata.js

ality by 1.0% agarose gel electrophoresis and

quantified by a NanoDrop 2000 (Thermo Fisher Scientific, Waltham, MA, USA). First-strand cDNA was synthesized from 1 µg of total RNA using a GoScript Reverse Transcription System (Promega). Primers specific to each of those selected genes were designed using Primer Express Software (version 3.0.1; Thermo Fisher Scientific), and *actin* was used as an endogenous reference gene (Table S1). Quantitative PCR (qPCR) was conducted using a StepOne Plus Real-Time PCR System (Thermo Fisher Scientific). Each reaction was 10 µL in volume that contained 5 µL of 2× EvaGreen qPCR Mastermix-ROX (Applied Biological Materials, Richmond, BC, Canada), 2 µL of 100× diluted cDNA templates and 3 µL of primer mixture (2.5 µM per primer). qPCR was conducted with the following program: 95°C for 10 min, 35 cycles of amplification at 95°C for 15 seconds and 60°C for 60 seconds. The relative expression of each selected gene was calculated according to the $2^{-\Delta\Delta C_T}$ method (Livak and Schmittgen 2001). Three biological replicates for each treatment were performed, in which three technical replicates were conducted for each biological replicate.

2.7 Data analysis

Data were statistically analyzed between two treatments using Student's *t*-test or determined among multiple treatments at each of assayed time points using Duncan's multiple range test of analysis of variance (ANOVA) by the SAS software (version 9.2; SAS Institute, Cary, NC, USA). To better elucidate the regulative roles of Se pretreatment on the plant responses to pathogen infection, the expression differentiation of the assayed genes was analyzed. Briefly, the differential expression was preliminarily elucidated the regulative effects induced by pathogen infection and Se pretreatment based on the pairwise analysis of In/Un or SeUn/Un. Thereafter, the expression differentiation of the pairwise Seln/In was further analyzed to understand the regulative effects of Se pretreatment during pathogen infection, which was excluded the regulative influence based on the expression differentiation of the pairwise Seln/Un.

3 Results

3.1 Lesion decreased by Se pretreatment

Lesions on leaves received 20, 40, and 60 µM Se pretreatment were significantly ($P < 0.05$) decreased 27.2%, 46.8%, and 39.0% compared to the control, respectively (Fig. 1). These results indicated that Se pretreatment can impact the disease progress caused by *S. sclerotiorum*. The 40 µM of Se pretreatment more efficiently reduced the lesion size. Thus, this concentration was selected for future analysis of necrotic development caused by *S. sclerotiorum*.

3.2 Se transformation and speciation in pretreated leaves

Total Se content in the sunflower leaves after Se pretreatment (SeUn) was 226.1 µg kg⁻¹, which was significantly ($P < 0.01$) higher (3.4-fold) compared to that without Se pretreatment (Un) (Fig. 2a). The

Loading [MathJax]/jax/output/CommonHTML/fonts/TeX/fontdata.js for standard selenocompounds of SeCys₂,

MeSeCys, selenite, SeMet, and selenate were approximately 172, 214, 262, 356, and 978 s, respectively (Fig. 2b). In this study, only two peaks (262 and 356 of retention times) were detected in Se pretreated leaves (SeUn), which matched with those of the standard selenite and SeMet (Fig. 2c). The contents of SeMet and selenite in the leaves of SeUn were $180.7 \mu\text{g kg}^{-1}$ and $13.7 \mu\text{g kg}^{-1}$, respectively. SeMet accounts for 79.9% of the total Se, which was the main Se speciation in the Se pretreated sunflower leaves (SeUn).

To evaluate the potential inhibitory effects of the detected Se speciation on fungal growth, mycelia growth of *S. sclerotiorum* was assessed on PDA supplied with each of detected Se speciation at their corresponding detected maximum concentration (i.e., $226.1 \mu\text{g L}^{-1}$) based on the analysis of total Se content and speciation in SeUn leaves. Our results indicated that both detected Se speciation did not affect mycelium growth of *S. sclerotiorum* (Fig. 2d). Therefore, Se and its transformed speciation detected in sunflower leaves after Se pretreatment did not directly inhibit the vegetative growth of *S. sclerotiorum*. This suggested that the impact on necrotic development caused by *S. sclerotiorum* infection were associated with plant responses induced by Se pretreatment, and were not derived from the inhibitory effect of Se.

3.3 Effects on necrotic development under Se pretreatment

Symptomatic lesions were observed at 12 hpi and gradually enlarged on the leaves challenged by *S. sclerotiorum* with (Seln) and without Se pretreatment (In) (Fig. 3a). The distinguished necrosis on the inoculated leaves under Seln and In was also validated by UV light observation (Fig. 3b). The lesion of the Seln treatment was not significantly different to that of In at 12 hpi, while the lesion of Seln was 38.5% less than that of In at 18 hpi. Subsequently, the lesion of Seln was 52.1% smaller than that of In at 24 hpi. Thereafter, the lesions derived from Seln significantly declined 54.4% and 51.3% compared to those of In at 36 and 48 hpi, respectively (Fig. 3c). According the necrosis development and lesion differentiation, three infection stages (i.e., 12, 24, and 36 hpi) were determined to further investigate the responses to *S. sclerotiorum* infection in this study. In addition, the necrosis development on sunflower leaves of Seln and In was further analyzed based on a logistic equation of time course of pathogenic development (Fig. 3d). Results indicated that the time course to reach the fastest rate of lesion expansion (50% of the final value) derived from Seln was 11 hours later than that of In (Table 1). The values of the slopes, including slope1 at the point of inflexion of the logistic curve and slope2 of the linear regression [i.e., $y'=-k(x-x_c)$], indicated that the rate of lesion development of Seln was slower than that of In. These results indicated that Se pretreatment reduced necrotic development caused by *S. sclerotiorum* infection on sunflower.

3.4 Regulation of redox homeostasis

The expression regulation of the crucial enzymes involved in redox homeostasis was investigated in a time course (e.g., 12, 24, and 36 hpi) of *S. sclerotiorum* infection (Fig. 4). Results indicated that the *cat* and *sod* expressions of In showed the decreased expression induced by pathogen infection (Fig. 4a and

Loading [MathJax]/jax/output/CommonHTML/fonts/TeX/fontdata.js ated 68.3%, 36.6%, and 64.0% compared to

those of Un at 12, 24, and 36 hpi, while the *cat* expressions of SeUn were significantly ($P < 0.05$) upregulated 1.5- and 2.0-fold than those of Un at 24 and 36 hpi (Fig. 4a). The *cat* expression of Seln was induced to be similar to the Un at 12 hpi, which showed a 2.5-fold increase compared to that of In (Fig. 4a). Our results indicated that the *cat* expression was decreased under pathogen infection, but was increased under Se pretreatment. Thus, Se pretreatment contributed to maintain the normal level (Un) of the *cat* expression at the earlier infection stage by upregulation of the *cat* expression. The *sod* expressions of In were consistently downregulated 72.3%, 59.4%, and 61.4% compared with those of Un at 12, 24, and 36 hpi, while those of SeUn were also significantly ($P < 0.05$) downregulated 66.3% and 45.5% than those of Un at 12 and 24 hpi (Fig. 4b). However, the *sod* expression showed no differential regulation between Seln and In at any assayed time points (Fig. 4b). Such results indicated that the *sod* expression was downregulated by either pathogen infection or Se pretreatment, but Se pretreatment was not involved in the *sod* expression regulation derived from pathogen infection in this study. These results indicated that the *cat* and *sod* expressions were decreased due to pathogen infection. Besides, *cat* expression was decreased due to Se pretreatment while *sod* expression was increased. Furthermore, Se pretreatment potentially increased the downregulation of *cat* expression caused by pathogen infection at the earlier infection stage.

The expression patterns of three genes (e.g., *apx*, *gpx* and *pod*) encoding ROS-scavenging enzymes were analyzed in this study. The *apx*, *gpx*, and *pod* expressions of In were significantly ($P < 0.05$) upregulated than those of Un, except for the *apx* expression at 36 hpi. For example, the *apx* expressions of In were significantly ($P < 0.05$) upregulated 2.1- and 2.0-fold than those of Un at 12 and 24 hpi, while the *apx* expression was not differentially regulated between SeUn and Un at any assayed time points (Fig. 4c). The *apx* expression of Seln was regulated to be similar to the Un at 24 hpi, which was 36.3% decreased compared to that of In (Fig. 4c). Similarly, the *gpx* expressions of In were consistently upregulated 1.9-, 6.7-, and 3.7-fold compared to those of Un at 12, 24, and 36 hpi. However, the *gpx* expressions of SeUn were not differentially regulated compared to those of Un at any assayed time points (Fig. 4d). The *gpx* expressions of Seln were significantly ($P < 0.05$) upregulated than those of Un at 24 and 36 hpi, but downregulated 45.7% and 42.5% compared to those of In (Fig. 4d). Furthermore, the *pod* expression patterns were similar to those of *gpx*. The *pod* expressions of In were significantly ($P < 0.05$) upregulated 3.0-, 4.3-, and 1.5-fold compared with those of Un at 12, 24, and 36 hpi. However, the *pod* expressions of SeUn were similar to those of Un at 12 and 24 hpi, which was downregulated 52.0% compared with that of Un at 36 hpi (Fig. 4e). The *pod* expressions of Seln were significantly ($P < 0.05$) upregulated than those of Un at 12 and 24 hpi, but 64.5% and 40.8% downregulation compared with those of In at 24 and 36 hpi (Fig. 4e). These results indicated that the *apx*, *gpx*, and *pod* expressions were increased due to pathogen infection, but not affected by Se pretreatment. However, Se pretreatment potentially played a regulative role to alleviate the increased expression caused by pathogen infection by downregulating the *apx*, *gpx*, and *pod* expressions at the later infection stage.

In addition, the *nox* expression of In was significantly ($P < 0.05$) upregulated 1.3-fold than that of Un at 36 hpi, while the *nox* expressions of SeUn were significantly ($P < 0.05$) downregulated 47.5% and 36.6% (Fig. 4f). The *nox* expression levels of Seln were

consistently downregulated than those of Un at any assayed time points, and significantly ($P < 0.05$) downregulated 51.1% and 56.5% compared to those of In at 24 and 36 hpi (Fig. 4f). These results indicated that the *nox* expressions were increased under pathogen infection, but were decreased under Se pretreatment. Thus, Se pretreatment downregulated the *nox* expressions, and played the regulative roles to alleviate the upregulation induced by pathogen infection at the later infection stage. Based on the expression analysis of these genes involved in redox homeostasis under Se pretreatment during pathogen infection, the regulative roles to alleviate the effects induced by Se pretreatment were elucidated based on the gene expression differentiation during pathogen infection, especially the upregulation of *cat* at the earlier infection stage (12 hpi), the downregulation of *apx*, *gpx*, and *pod* at the developing infection stage (24 hpi), and the downregulation of *gpx* and *nox* at the later infection stages (36 hpi).

3.5 Regulation of plant hormone signaling pathways

The expression regulation of the critical genes involved to signaling pathway was also analyzed at 12, 24, and 36 hpi (Fig. 5). The *AOC* expression of In were significantly ($P < 0.05$) upregulated 13.5-, 9.0-, and 12.9-fold compared to those of Un at 12, 24, and 36 hpi, while *AOC* expression was not differentially regulated between SeUn and Un at any assayed time points (Fig. 5a). *AOC* expressions of Seln were significantly upregulated than those of Un, and increased 2.0- and 2.7-fold than those of In at 12 and 24 hpi, respectively (Fig. 5a). The *PDF* expressions of In were also significantly ($P < 0.05$) upregulated 2.7-, 3.0-, and 5.9-fold than those of Un at 12, 24, and 36 hpi, respectively, while the *PDF* expression of SeUn was significantly ($P < 0.05$) upregulated 4.4-fold than that of Un at 12 hpi (Fig. 5b). The *PDF* expression of Seln was significantly upregulated than those of Un, and increased 1.8-fold than that of In at 24 hpi (Fig. 5b). The *PAL* expressions of In were consistently upregulated 1.9-, 3.3-, and 4.5-fold than those of Un at 12, 24, and 36 hpi, while the *PAL* expression of SeUn was not differentially regulated compared to that of Un (Fig. 5c). The *PAL* expressions of Seln were significantly ($P < 0.05$) upregulated than those of Un at any assayed time points, while increased 1.5-fold at 12 hpi and decreased at 36 hpi than that of In (Fig. 5c). These results indicated that the *AOC*, *PDF*, and *PAL* expressions were increased by pathogen infection, and were not significantly regulated by Se pretreatment. However, Se pretreatment potentially played regulative roles to alleviate the upregulation of the *AOC*, *PDF*, and *PAL* expressions induced by pathogen infection during all of infection stage.

The *EIN2* expressions of In were consistently downregulated 42.0%, 56.4%, and 36.0% compared with those of Un at 12, 24, and 36 hpi, while the *EIN2* expressions of SeUn were significantly ($P < 0.05$) upregulated 1.4- and 2.1-fold than those of Un at 12 and 24 hpi (Fig. 5d). The *EIN2* expressions of Seln were consistently not changed compared to those of Un at 12, 24, and 36 hpi, and upregulated 1.8-, 2.0-, and 1.5-fold than those of In (Fig. 5d). These results indicated that the *EIN2* expression was decreased under pathogen infection, and was increased under Se pretreatment. Thus, Se pretreatment contributed to maintain the normal level (Un) of the *EIN2* expression at all of infection stage by upregulation of *EIN2* expression. According to the expression analysis of the curial genes involved in hormonal signaling pathways under Se pretreatment during pathogen infection, the roles of Se pretreatment were elucidated.

Se pretreatment upregulated *AOC*, *PAL*, and *EIN2* at the earlier infection stage (12 hpi) and upregulated *AOC*, *PDF*, and *EIN2* at the developing infection stage (24 hpi), while downregulated *PDF* and *PAL* and upregulated *EIN2* at the later infection stage (36 hpi).

4 Discussion

Nutrient elements (e.g., Se) are frequently applied on plant to improve growth and disease resistance (Dordas 2008; Feng et al. 2013). In previous studies, Se was used as a protective chemical on mustard against *Fusarium* species as well as *B. cinerea* and *Alternaria solani* infection on tomato (Hanson et al. 2003; Quiterio-Gutiérrez et al. 2019; Wu et al. 2016). Our results showed that Se pretreatment delayed the lesion occurrence and slowed the necrosis expansion on sunflower leaves. Se content in the Se-pretreated sunflower leaves was detected mainly as the form of SeMet. SeMet is more active than selenite and can incorporate into proteins nonspecifically through the metabolic pathways of sulfur analogues by replacing Met to the form of Se-containing proteins (Wu et al. 2020; Zhang et al. 2020). In plants, Se-containing proteins not only carry enzymatic functions, but also carry antioxidant activity by scavenging free radicals directly (Liu et al. 2015; Zhang et al. 2020).

Activation of plant resistance to pathogen infection has been found to be a result of complex mechanisms, with the involvement of redox homeostasis regulation and plant hormone signaling pathways (Bari and Jones 2009; Torres et al. 2006). For example, sunflower seeds pre-soaked with Se weakened the oxidative damage caused by cadmium (Saidi et al. 2014). Thereby, the regulations of genes associated with redox homeostasis and plant hormone signaling pathways were assessed in Se pretreated sunflower after challenge by *S. sclerotiorum*. Expression analysis indicated the coordinated regulation between Se and the pathogen. Interacting with the regulatory effects caused by *S. sclerotiorum* infection, Se pretreatment increased the downregulation of *cat* and decreased the upregulation of *apx*, *gpx*, *pod*, and *nox* at the different infection stages. In a previous study, upregulation of *cat* in sunflower was found to be able to improve resistance to *S. sclerotiorum* (Na et al. 2018). In another study, the downregulation of *pod* and *apx* in tomato by the treatment of manganese phosphite could reduce the disease severity caused by *S. sclerotiorum* (Chaves et al. 2021). The downregulation of *sod* expression was previously found to improve soybean resistance to *S. sclerotiorum* after sprayed with calcium (Arfaoui et al. 2018). However, in this study, Se pretreatment did not affect the downregulation of *sod* expression in sunflower infected by *S. sclerotiorum*. Thus, the mechanism of Se pretreatment affecting *sod* expression might be different. In addition, the activated response dependent on *nox* regulation perturbed the disease progress of *S. sclerotiorum* in Arabidopsis (Zhou et al. 2013). Our results suggested that Se pretreatment contributed to the coordinated regulation of redox homeostasis by alleviating ROS during the disease development of *S. sclerotiorum* in sunflowers.

Plant signaling pathways are involved in the regulation of plant defense responses, particularly the JA, ET, and SA pathways (Yang et al. 2015). For example, melatonin was found to promote tomato resistance to *B. cinerea* through regulating H₂O₂ accumulation and JA signaling pathway (Liu et al. 2019). In this

Loading [MathJax]/jax/output/CommonHTML/fonts/TeX/fontdata.js the ET signaling pathway, and *PAL* in the SA

signaling pathway were significantly upregulated in the Se pretreated sunflower inoculated by *S. sclerotiorum*. In a previous study, upregulated expressions of *AOC* and *PDF* in the JA pathway was found in oilseed rape after infected by *S. sclerotiorum* (Zhao et al. 2009). Similarly, the *AOC* expression was significantly enhanced in mustard infected by *S. sclerotiorum*, while *PDF* was able to improve Arabidopsis resistance against *A. brassicicola* (Penninckx et al. 1998; Yang et al. 2010). In addition, *PAL* expression in tomato was upregulated as a response of *S. sclerotiorum* infection (Farzand et al. 2019). *EIN2* expression was upregulated as the defense responses to *S. sclerotiorum* in Arabidopsis (Guo and Stotz 2007). Therefore, Se pretreatment contributed to the resistant improvement by coordinately regulating plant hormone signaling pathways during the infection process of *S. sclerotiorum*.

A model that Se pretreatment modulated the responses to *S. sclerotiorum* infection was proposed for crosstalk between redox homeostasis and plant hormone signaling pathways (Fig. 6). Based on the evidence of our analysis, this model illuminates the contribution by Se on the improvement of sunflower resistance to *S. sclerotiorum* and perhaps in other plant pathosystems. According to the regulation of gene expressions, the redox homeostasis in sunflower responded to *S. sclerotiorum* infection was alleviated by the Se application. In other studies, Se was also found to mitigate the damage of ROS under cadmium stress in rice (Xu et al. 2020). Iron oxide nanoparticles regulated the antioxidant defense to maintain redox homeostasis in Moldavian dragonhead under salinity stress (Moradbeygi et al. 2020). Plant signaling pathways were also associated with the regulation of redox homeostasis (Overmyer et al. 2003). Overall, we proposed that Se coordinated the regulation of redox homeostasis and signaling pathways to improve resistance to *S. sclerotiorum*. This study provided a new clue for the sustainable management of Sclerotinia wilt on sunflower by Se foliar application.

Declarations

Ethics approval and consent to participate

Not applicable.

Consent for publication

Not applicable.

Availability of data and materials

All data generated or analyzed during this study are included in this published article and its supplementary information files.

Competing interests

No conflict of interest declared.

Funding

Loading [MathJax]/jax/output/CommonHTML/fonts/TeX/fontdata.js

This work was supported by the Special Fund for Agro-scientific Research in the Public Interest (201303106), the National Natural Science Foundation of China (31470531), LiaoNing Revitalization Talents Program (XLYC1807242), and the Scientific Research Foundation for the Introduced Talents of Shenyang Agricultural University (20153040).

Authors' contributions

YG and YL: Conceived and designed the experiments; ZC, HS, TH, and ZW: Performed the experiments; ZC, YL, and YG: Analyzed the data and wrote the manuscript; YG, YL, and WW: Revised and improved the manuscript. All authors read and approved the final manuscript.

References

- Alagawany M, Farag MR, El-Hack MEA, Dhama K (2015) The practical application of sunflower meal in poultry nutrition. *Adv Anim Vet Sci* 3: 634-648. <https://doi.org/10.14737/journal.aavs/2015/3.12.634.648>
- Arfaoui A, El Hadrami A, Daayf F (2018) Pre-treatment of soybean plants with calcium stimulates ROS responses and mitigates infection by *Sclerotinia sclerotiorum*. *Plant Physiol Bioch* 122: 121-128. <https://doi.org/10.1016/j.plaphy.2017.11.014>
- Bañuelos GS, Lin ZQ, Broadley M (2017) Selenium Biofortification. In: Pilon-Smits EAH (ed) *Selenium in plants*. Springer, Berlin, pp 231-255.
- Bari R, Jones JD (2009) Role of plant hormones in plant defence responses. *Plant Mol Biol* 69: 473-488. <https://doi.org/10.1007/s11103-008-9435-0>
- Bolton MD, Thomma BP, Nelson BD (2006) *Sclerotinia sclerotiorum* (Lib.) de Bary: biology and molecular traits of a cosmopolitan pathogen. *Mol Plant Pathol* 7: 1-16. <https://doi.org/10.1111/j.1364-3703.2005.00316.x>
- Boyd RS (2007) The defense hypothesis of elemental hyperaccumulation: status, challenges and new directions. *Plant Soil* 293: 153-176. <https://doi.org/10.1007/s11104-007-9240-6>
- Chaves JAA, Oliveira LM, Silva LC, Silva BN, Dias CS, Rios JA, Rodrigues FÁ (2021) Physiological and biochemical responses of tomato plants to white mold affected by manganese phosphite. *J Phytopathol* 169: 149-167. <https://doi.org/10.1111/jph.12969>
- Debaeke P, Mestries E, Desanlis M, Seassau C (2014) Effects of crop management on the incidence and severity of fungal diseases in sunflower. In: Arribas JI (ed) *Sunflowers: growth and development, environmental influences and pests/diseases*. Nova Science Pubs, New York, pp 201-226.
- Dordas C (2008) Role of nutrients in controlling plant diseases in sustainable agriculture. A review. *Agron Sustain Dev* 28: 33-46. <https://doi.org/10.1051/agro:2007051>

- Ekins MG, Hayden HL, Aitken EAB, Goulter KC (2011) Population structure of *Sclerotinia sclerotiorum* on sunflower in Australia. *Australasian Plant Pathol* 40: 99-108. <https://doi.org/10.1007/s13313-010-0018-6>
- El-Ramady HR, Domokos-Szabolcsy É, Abdalla NA, Alshaal TA, Shalaby TA, Sztrik A, Prokisch J, Fári M (2014) Selenium and nano-selenium in agroecosystems. *Environ Chem Lett* 12: 495-510. <https://doi.org/10.1007/s10311-014-0476-0>
- Fagundes-Nacarath IRF, Debona D, Rodrigues FA (2018) Oxalic acid-mediated biochemical and physiological changes in the common bean-*Sclerotinia sclerotiorum* interaction. *Plant Physiol Bioch* 129: 109-121. <https://doi.org/10.1016/j.plaphy.2018.05.028>
- FAOSAT, Food and Agriculture data, <http://www.fao.org/faostat/>, (2020) (Accessed December 22, 2020)
- Farooq M, Tang Z, Zeng R, Liang Y, Zhang Y, Zheng T, Ei HH, Ye X, Jia X, Zhu J (2019) Accumulation, mobilization, and transformation of selenium in rice grain provided with foliar sodium selenite. *J Sci Food Agric* 99: 2892-2900. <https://doi.org/10.1002/jsfa.9502>
- Farzand A, Moosa A, Zubair M, Khan AR, Massawe VC, Tahir HAS, Sheikh TMM, Ayaz M, Gao X (2019) Suppression of *Sclerotinia sclerotiorum* by the induction of systemic resistance and regulation of antioxidant pathways in tomato using Fengycin produced by *Bacillus amyloliquefaciens* FZB42. *Biomolecules* 9: 613. <https://doi.org/10.3390/biom9100613>
- Feng R, Wei C, Tu S (2013) The roles of selenium in protecting plants against abiotic stresses. *Environ Exp Bot* 87: 58-68. <https://doi.org/10.1016/j.envexpbot.2012.09.002>
- Fujita M, Fujita Y, Noutoshi Y, Takahashi F, Narusaka Y, Yamaguchi-Shinozaki K, Shinozaki K (2006) Crosstalk between abiotic and biotic stress responses: a current view from the points of convergence in the stress signaling networks. *Curr Opin Plant Biol* 9: 436-442. <https://doi.org/10.1016/j.pbi.2006.05.014>
- Guo S, Ge Y, Jom KN (2017) A review of phytochemistry, metabolite changes, and medicinal uses of the common sunflower seed and sprouts (*Helianthus annuus* L.). *Chem Cent J* 11: 95. <https://doi.org/10.1186/s13065-017-0328-7>
- Guo X, Stotz HU (2007) Defense against *Sclerotinia sclerotiorum* in *Arabidopsis* is dependent on jasmonic acid, salicylic acid, and ethylene signaling. *Mol Plant Microbe In* 20: 1384-1395. <https://doi.org/10.1094/MPMI-20-11-1384>
- Hanson B, Garifullina GF, Lindblom SD, Wangeline A, Ackley A, Kramer K, Norton AP, Lawrence CB, Pilon-Smits EAH (2003) Selenium accumulation protects *Brassica juncea* from invertebrate herbivory and fungal infection. *New Phytol* 159: 461-469. <https://doi.org/10.1046/j.1469-8137.2003.00786.x>
- Hu T, Li H, Li J, Zhao G, Wu W, Liu L, Wang Q, Guo Y (2018) Absorption and bio-transformation of selenium nanoparticles by wheat seedlings (*Triticum aestivum* L.). *Front Plant Sci* 9.

- Kápolna E, Hillestrom PR, Laursen KH, Husted S, Larsen EH (2009) Effect of foliar application of selenium on its uptake and speciation in carrot. *Food Chem* 115: 1357-1363.
<https://doi.org/10.1016/j.foodchem.2009.01.054>
- Kim KS, Min JY, Dickman MB (2008) Oxalic acid is an elicitor of plant programmed cell death during *Sclerotinia sclerotiorum* disease development. *Mol Plant Microbe In* 21: 605-612.
<https://doi.org/10.1094/MPMI-21-5-0605>
- Li Q, Ai G, Shen D, Zou F, Wang J, Bai T, Chen Y, Li S, Zhang M, Jing M, Dou D (2019) A *Phytophthora capsici* effector targets ACD11 binding partners that regulate ROS-mediated defense response in *Arabidopsis*. *Mol Plant* 12: 565-581. <https://doi.org/10.1016/j.molp.2019.01.018>
- Liang XF, Jeffrey, AR (2018) Mechanisms of broad host range necrotrophic pathogenesis in *Sclerotinia sclerotiorum*. *Phytopathology* 108: 1128-1140. <http://doi.org/10.1094/PHYTO-06-18-0197-RVW>
- Liang Y, Strelkov SE, Kav NNV (2009) Oxalic acid-mediated stress responses in *Brassica napus* L. *Proteomics* 9: 3156-3173. <https://doi.org/10.1002/pmic.200800966>
- Liang Y, Xiong W, Steinkellner S, Feng J (2018) Deficiency of the melanin biosynthesis genes *SCD1* and *THR1* affects sclerotial development and vegetative growth, but not pathogenicity, in *Sclerotinia sclerotiorum*. *Mol Plant Pathol* 19: 1444-1453. <https://doi.org/10.1111/mpp.12627>
- Liu C, Chen L, Zhao R, Li R, Zhang S, Yu W, Sheng J, Shen L (2019) Melatonin induces disease resistance to *Botrytis cinerea* in tomato fruit by activating jasmonic acid signaling pathway. *J Agr Food Chem* 67: 6116-6124. <https://doi.org/10.1021/acs.jafc.9b00058>
- Liu J, Zhang Y, Meng Q, Shi F, Ma L, Li Y (2017) Physiological and biochemical responses in sunflower leaves infected by *Sclerotinia sclerotiorum*. *Physiol Mol Plant P* 100: 41-48.
<https://doi.org/10.1016/j.pmpp.2017.06.001>
- Liu K, Zhao Y, Chen F, Fang Y (2015) Purification and identification of Se-containing antioxidative peptides from enzymatic hydrolysates of Se-enriched brown rice protein. *Food Chem* 187: 424-430.
<https://doi.org/10.1016/j.foodchem.2015.04.086>
- Livak KJ, Schmittgen TD (2001) Analysis of relative gene expression data using real-time quantitative PCR and the method. *Methods* 25: 402-408. <https://doi.org/10.1006/meth.2001>
- Ma L, Zhang Y, Meng Q, Shi F, Liu J, Li Y (2018) Enhancement of *Sclerotinia sclerotiorum* and oxalic acid resistance in tobacco by a novel pathogen-induced GST gene from sunflower. *Crop Sci* 58: 1318-1327.
<https://doi.org/10.2135/cropsci2017.08.0479>
- Moradbeygi H, Jamei R, Heidari R, Darvishzadeh R (2020) Investigating the enzymatic and non-enzymatic antioxidant defense by applying iron oxide nanoparticles in *Dracocephalum moldavica* L. plant under
<https://doi.org/10.1016/j.scienta.2020.109537>

- Na R, Luo Y, Bo H, Zhang J, Jia R, Meng Q, Zhou H, Hao J, Zhao J (2018) Response of sunflower induced by *Sclerotinia sclerotiorum* infection. *Physiol Mol Plant P* 102: 113-121. <https://doi.org/10.1016/j.pmpp.2017.12.004>
- Nováková M, Šásek V, Dobrev PI, Valentová O, Burketová L (2014) Plant hormones in defense response of *Brassica napus* to *Sclerotinia sclerotiorum* – reassessing the role of salicylic acid in the interaction with a necrotroph. *Plant Physiol Bioch* 80: 308-317. <https://doi.org/10.1016/j.plaphy.2014.04.019>
- Overmyer K, Brosché M, Kangasjärvi J (2003) Reactive oxygen species and hormonal control of cell death. *Trends Plant Sci* 8: 335-342. [https://doi.org/10.1016/S1360-1385\(03\)00135-3](https://doi.org/10.1016/S1360-1385(03)00135-3)
- Penninckx IAMA, Thomma BPHJ, Buchala A, Métraux JP, Broekaert WF (1998) Concomitant activation of jasmonate and ethylene response pathways is required for induction of a plant defensin gene in *Arabidopsis*. *Plant Cell* 10: 2103-2113. <https://doi.org/10.1105/tpc.10.12.2103>
- Quiterio-Gutiérrez T, Ortega-Ortiz H, Cadenas-Pliego G, Hernández-Fuentes AD, Sandoval-Rangel A, Benavides-Mendoza A, Cabrera-de la Fuente M, Juárez-Maldonado A (2019) The application of selenium and copper nanoparticles modifies the biochemical response of tomato plants under stress by *Alternaria solani*. *Int J Mol Sci* 20: 1950. <https://doi.org/10.3390/ijms20081950>
- Ranjan A, Jayaraman D, Grau C, Hill JH, Whitham SA, Ané JM, Smith DL, Kabbage M (2018) The pathogenic development of *Sclerotinia sclerotiorum* in soybean requires specific host NADPH oxidases. *Mol Plant Pathol* 19: 700-714. <https://doi.org/10.1111/mp.12555>
- Saidi I, Chtourou Y, Djebali W (2014) Selenium alleviates cadmium toxicity by preventing oxidative stress in sunflower (*Helianthus annuus*) seedlings. *J Plant Physiol* 171: 85-91. <https://doi.org/10.1016/j.jplph.2013.09.024>
- Seiler GJ, Qi LL, Marek LF (2017) Utilization of sunflower crop wild relatives for cultivated sunflower improvement. *Crop Sci* 57: 1083-1101. <https://doi.org/10.2135/cropsci2016.10.0856>
- Sharma P, Sharma P, Arora P, Verma V, Khanna K, Saini P, Bhardwaj R (2019) Role and regulation of ROS and antioxidants as signaling molecules in response to abiotic stresses. In: Khan MIR (ed) *Plant Signaling Molecules*. Woodhead, Cambridge, pp 141-156. <https://doi.org/10.1016/B978-0-12-816451-8.00008-3>
- Spoel SH, Dong X (2008) Making sense of hormone crosstalk during plant immune responses. *Cell Host Microbe* 3: 348-351. <https://doi.org/10.1016/j.chom.2008.05.009>
- Suzuki N, Miller G, Morales J, Shulaev V, Torres MA, Mittler R (2011) Respiratory burst oxidases: the engines of ROS signaling. *Curr Opin Plant Biol* 14: 691-699. <https://doi.org/10.1016/j.pbi.2011.07.014>
- Tiwari S, Tiwari S, Singh M, Singh A, Prasad SM (2017) Generation mechanisms of reactive oxygen

- Revisiting the Role of Reactive Oxygen Species (ROS) in Plants: ROS Boon or Bane for Plants. Wiley, New York, pp. 1-22.
- Torres MA, Jones JD, Dangl JL (2006) Reactive oxygen species signaling in response to pathogens. *Plant Physiol* 141: 373-378. <https://doi.org/10.1104/pp.106.079467>
- Toscano S, Romano D, Tribulato A, Patanè C (2017) Effects of drought stress on seed germination of ornamental sunflowers. *Acta Physiol Plant* 39: 184. <https://doi.org/10.1007/s11738-017-2484-8>
- Wang K, Wang Y, Li K, Wan Y, Wang Q, Zhuang Z, Guo Y, Li H (2020) Uptake, translocation and biotransformation of selenium nanoparticles in rice seedlings (*Oryza sativa* L.). *J Nanobiotechnol* 18: 103. <https://doi.org/10.1186/s12951-020-00659-6>
- Wang Z, Mao H, Dong C, Ji R, Cai L, Fu H, Liu S (2009) Overexpression of *Brassica napus* MPK4 enhances resistance to *Sclerotinia sclerotiorum* in oilseed rape. *Mol Plant Microbe In* 22: 235-244. <https://doi.org/10.1094/MPMI-22-3-0235>
- Williams B, Kabbage M, Kim HJ, Britt R, Dickman MB (2011) Tipping the balance: *Sclerotinia sclerotiorum* secreted oxalic acid suppresses host defenses by manipulating the host redox environment. *PLoS Pathog* 7: e1002107. <https://doi.org/10.1371/journal.ppat.1002107>
- Winkel LH, Vriens B, Jones GD, Schneider LS, Pilon-Smits E, Bañuelos GS (2015) Selenium cycling across soil-plant-atmosphere interfaces: a critical review. *Nutrients* 7: 4199-4239. <https://doi.org/10.3390/nu7064199>
- Wu Z, Yin X, Bañuelos GS, Lin ZQ, Zhu Z, Liu Y, Yuan L, Li M (2016) Effect of selenium on control of postharvest gray mold of tomato fruit and the possible mechanisms involved. *Front Microbiol* 6: 1441. <https://doi.org/10.3389/fmicb.2015.01441>
- Wu M, Cong X, Li M, Rao S, Liu Y, Guo J, Zhu S, Chen S, Xu F, Cheng S, Liu L, Yu T (2020) Effects of different exogenous selenium on Se accumulation, nutrition quality, elements uptake, and antioxidant response in the hyperaccumulation plant *Cardamine violifolia*. *Ecotox Environ Safe* 204: 111045. <https://doi.org/10.1016/j.ecoenv.2020.111045>
- Xia XJ, Zhou YH, Shi K, Zhou J, Foyer CH, Yu JQ (2015) Interplay between reactive oxygen species and hormones in the control of plant development and stress tolerance. *J Exp Bot* 66: 2839-2856. <https://doi.org/10.1093/jxb/erv089>
- Xu H, Yan J, Qin Y, Xu J, Shohag MJI, Wei Y, Gu M (2020) Effect of different forms of selenium on the physiological response and the cadmium uptake by rice under cadmium stress. *Int J Env Res Pub He* 17: 6991. <https://doi.org/10.3390/ijerph17196991>

Yang B, Rahman MH, Liang Y, Shah S, Kav NN (2010) Characterization of defense signaling pathways of *Sclerotinia sclerotiorum* challenge. *Plant Mol Biol*

Yang YX, Ahammed GJ, Wu C, Fan S, Zhou YH (2015) Crosstalk among jasmonate, salicylate and ethylene signaling pathways in plant disease and immune responses. *Curr Protein Pept Sc* 16: 450-461. <https://doi.org/10.2174/1389203716666150330141638>

Zhang X, He H, Xiang J, Yin H, Hou T (2020) Selenium-containing proteins/peptides from plants: A review on the structures and functions. *J Agr Food Chem* 68: 15061-15073. <https://dx.doi.org/10.1021/acs.jafc.0c05594>

Zhao J, Buchwaldt L, Rimmer SR, Sharpe A, McGregor L, Bekkaoui D, Hegedus D (2009) Patterns of differential gene expression in *Brassica napus* cultivars infected with *Sclerotinia sclerotiorum*. *Mol Plant Pathol* 10: 635-649. <https://doi.org/10.1111/j.1364-3703.2009.00558.x>

Zhou J, Sun A, Xing D (2013) Modulation of cellular redox status by thiamine-activated NADPH oxidase confers Arabidopsis resistance to *Sclerotinia sclerotiorum*. *J Exp Bot* 64: 3261-3272. <https://doi.org/10.1093/jxb/ert166>

Tables

Table 1 Logistic analysis of lesion development after inoculation

| Treatment | $y = \frac{a}{1 + e^{-k(x-x_c)}}$ † | x_c | Slope1 | Slope2 | Adjusted r^2 |
|-----------|---|-------|--------|--------|----------------|
| SeIn | $y = \frac{10}{1 + e^{-0.09(x-53.92)}}$ | 53.92 | 0.23 | -0.09 | 0.97 |
| In | $y = \frac{10}{1 + e^{-0.12(x-42.78)}}$ | 42.78 | 0.30 | -0.12 | 0.93 |

† Logistic function was fitted to the data of lesion size against time and lesion size (y) was regressed on time (x) from inoculation. Parameters: a (10 cm^2) defined final value of y , x_c , time (hours) until 50% of this final value was reached, *Slope1*, slope at time x_c , *Slope2*, slope of the linear regression (i.e., $y' = -k(x-x_c)$) of logistic function.

Figures

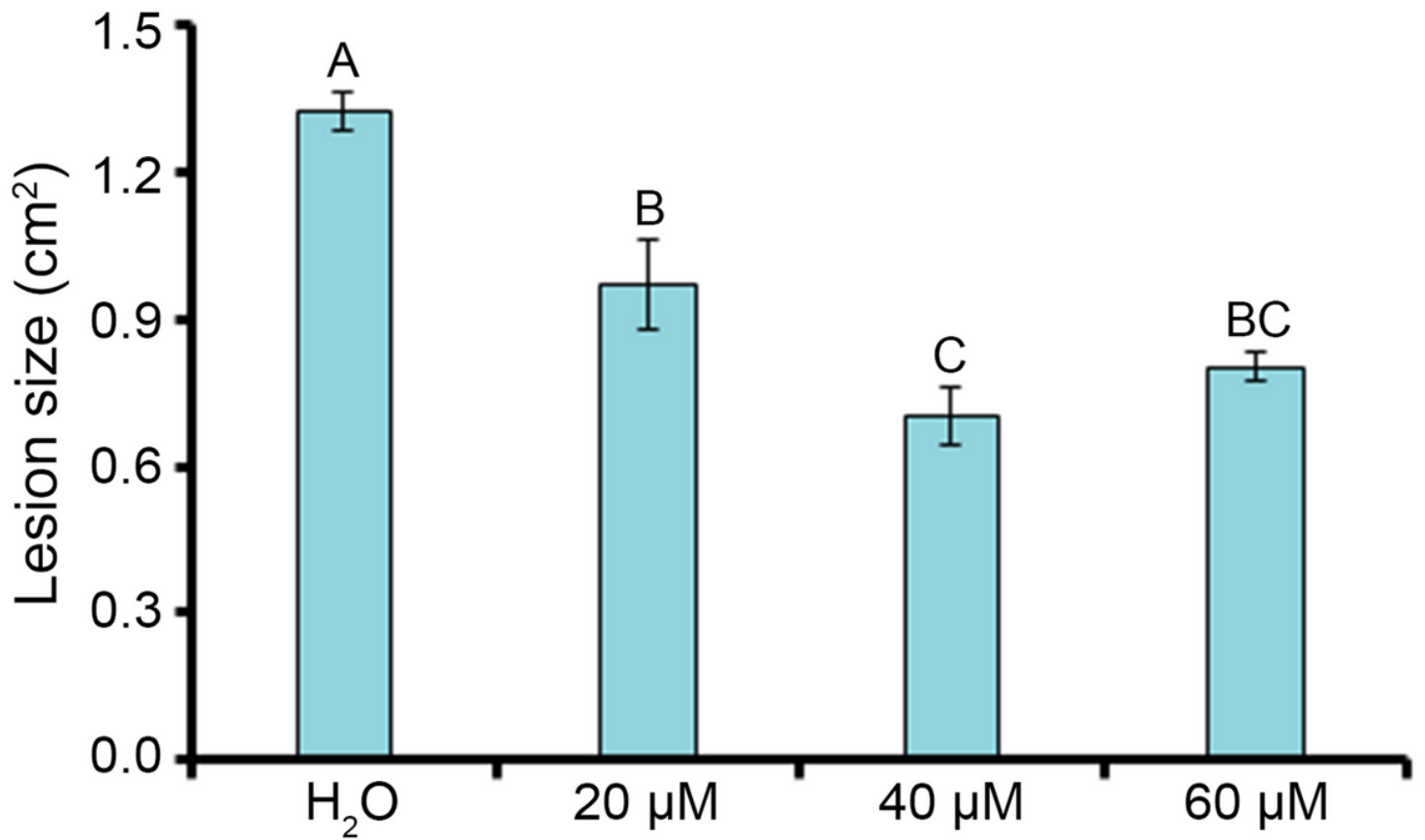


Figure 1

Lesion size on sunflower leaves after pre-treatment with Se and then inoculated with *S. sclerotiorum*. Data is shown as mean \pm standard error. Means in the plot topped by the same letter do not differ based on Duncan's multiple range test at $P < 0.05$ ($n = 3$).

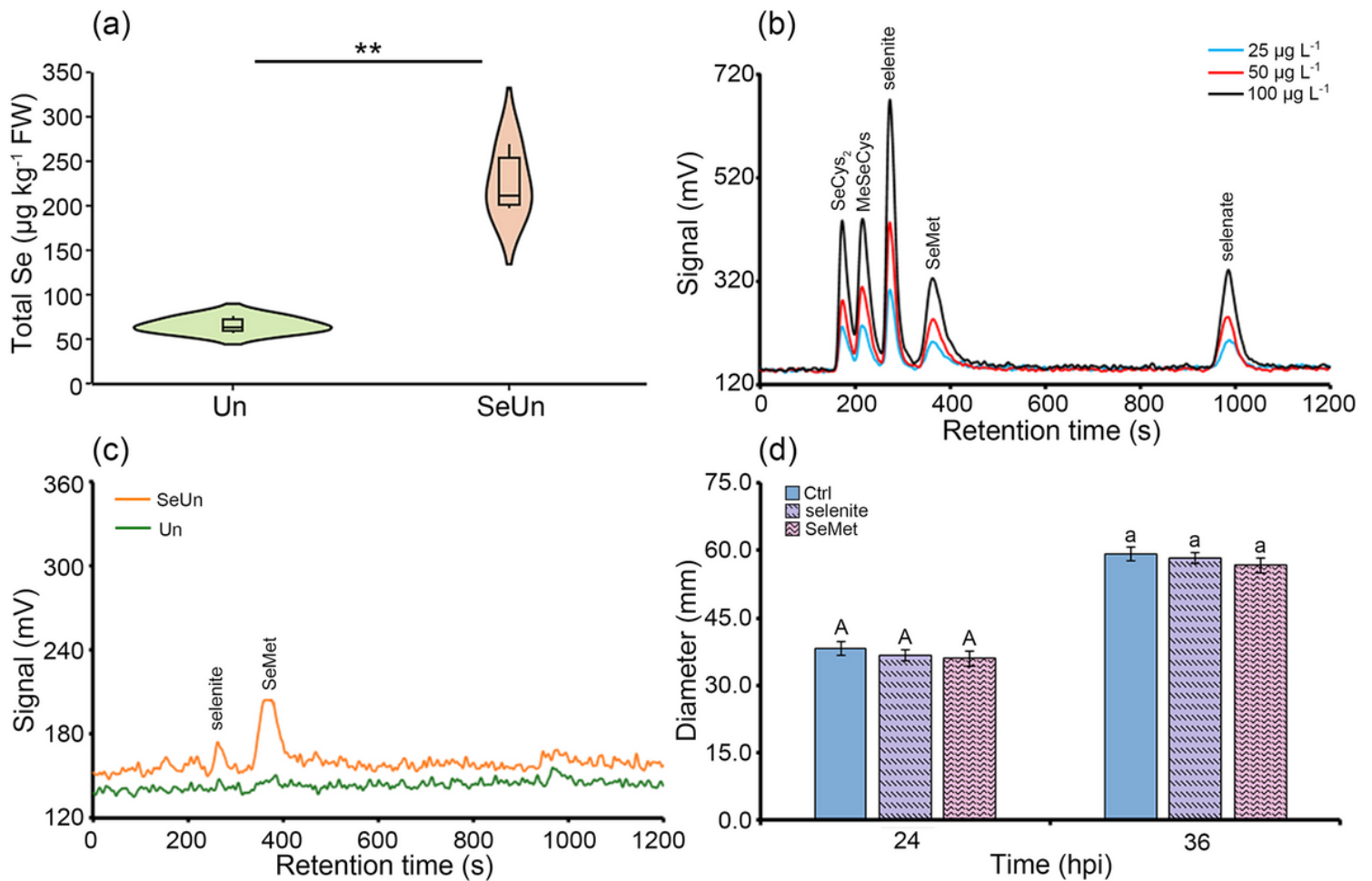


Figure 2

Total Se content and Se speciation of sunflower leaves. (a) Accumulation of Se in sunflower leaves 3 days after foliar application of Se. Se content was analyzed between the healthy leaves with (SeUn) and without Se treatment (Un) with the Student's t-test (**, $P < 0.01$). (b) Chromatogram of 5 standard selenocompounds at 25, 50, and 100 $\mu\text{g L}^{-1}$ of Se. (c) Examples of chromatograms of Se speciation in sunflower leaves with (SeUn) or without Se treatment (Un). (d) Effect of selenite and SeMet on the in vitro growth of *S. sclerotiorum* in the absence of sunflower. Diameters were measured at 24 and 36 hpi. Data are means \pm standard error. Diameters were statistically analyzed by ANOVA with Duncan's multiple range test ($P < 0.05$) at a specific time point. Means in the plot topped by the same letter do not differ based on Duncan's multiple range test at $P < 0.05$ ($n = 3$) (the capital for the 24 hpi and the lower case for the 36 hpi).

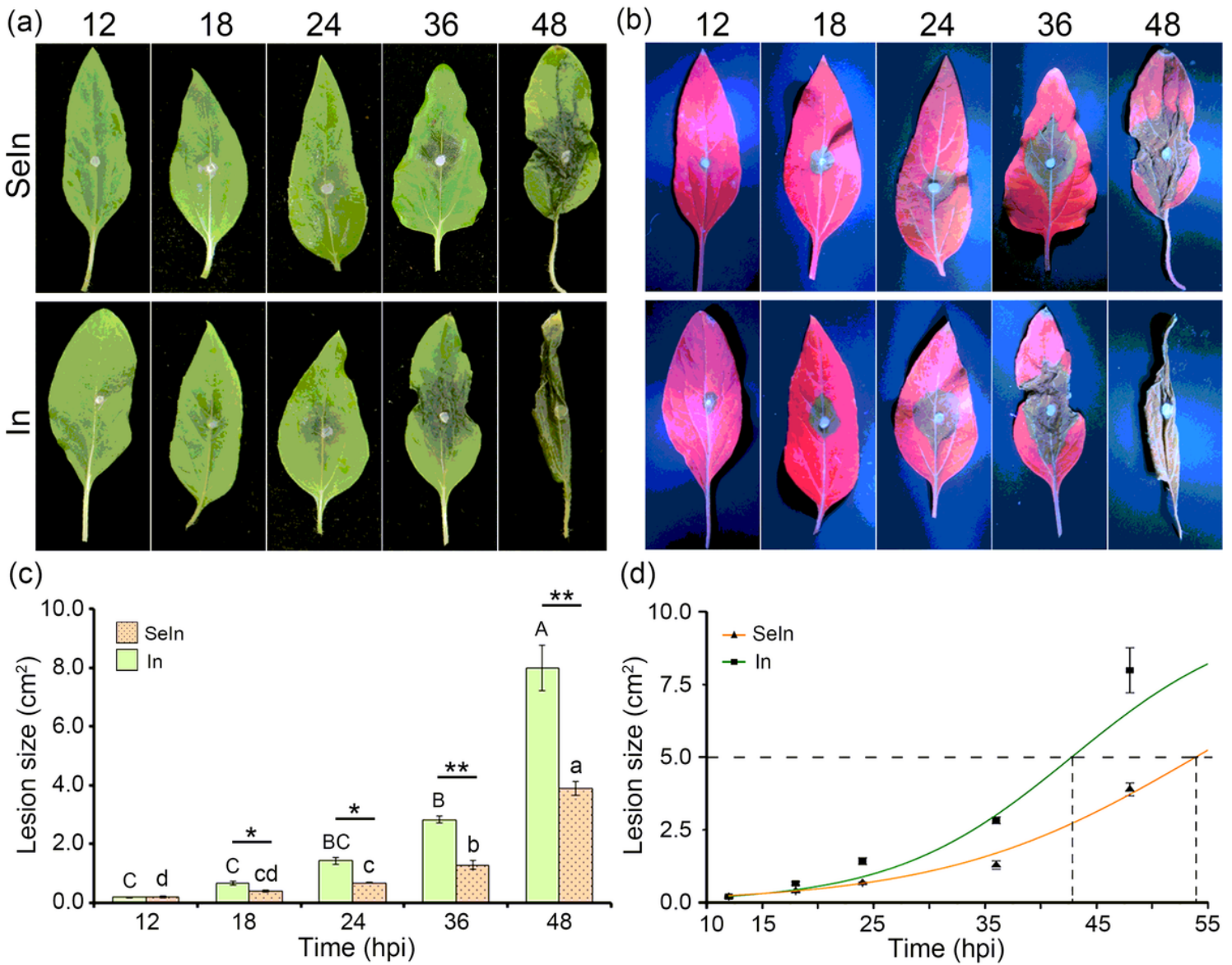


Figure 3

Appearance of sunflower leaves inoculated with *S. sclerotiorum* with Se treatment (Seln) and the inoculated plants without Se treatment (In). Photographs were taken at 12, 18, 24, 36, and 48 hpi under visible (a) and UV light (b). Lesion size on sunflower leaves (c). Data are means \pm standard error. Lesion caused by the pathogen inoculation with (Seln) and without (In) Se treatment among the assayed time points were statistically analyzed by ANOVA with Duncan's multiple range test ($P < 0.05$) while those at a specific time point between the Seln and In were evaluated by the Student's t-test (*, $P < 0.05$ and **, $P < 0.01$). For each treatment, means in the plot topped by the different letters indicate significant differences (the capital for the In and the lower case for the Seln). (d) Logistic function was fitted to the data of lesion size against time and lesion size (y) was regressed on time (x) from inoculation.

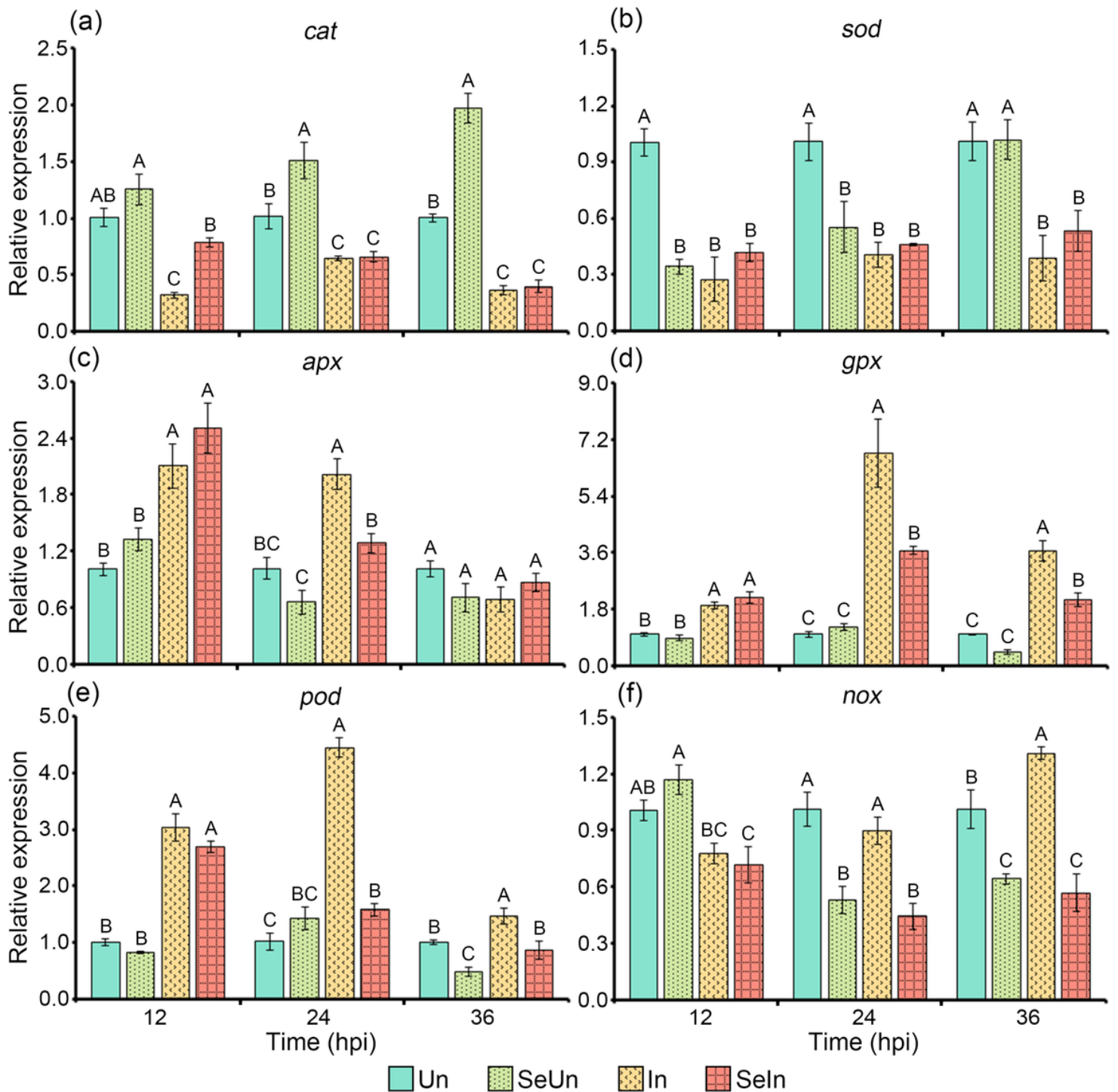


Figure 4

Evaluation of pathogen- or Se-mediated changes in transcript levels of enzymatic genes involved in redox homeostasis. Data is shown as mean \pm standard error. Means in the plot topped by the same letter do not differ based on Duncan's multiple range test at $P < 0.05$ ($n = 3$).

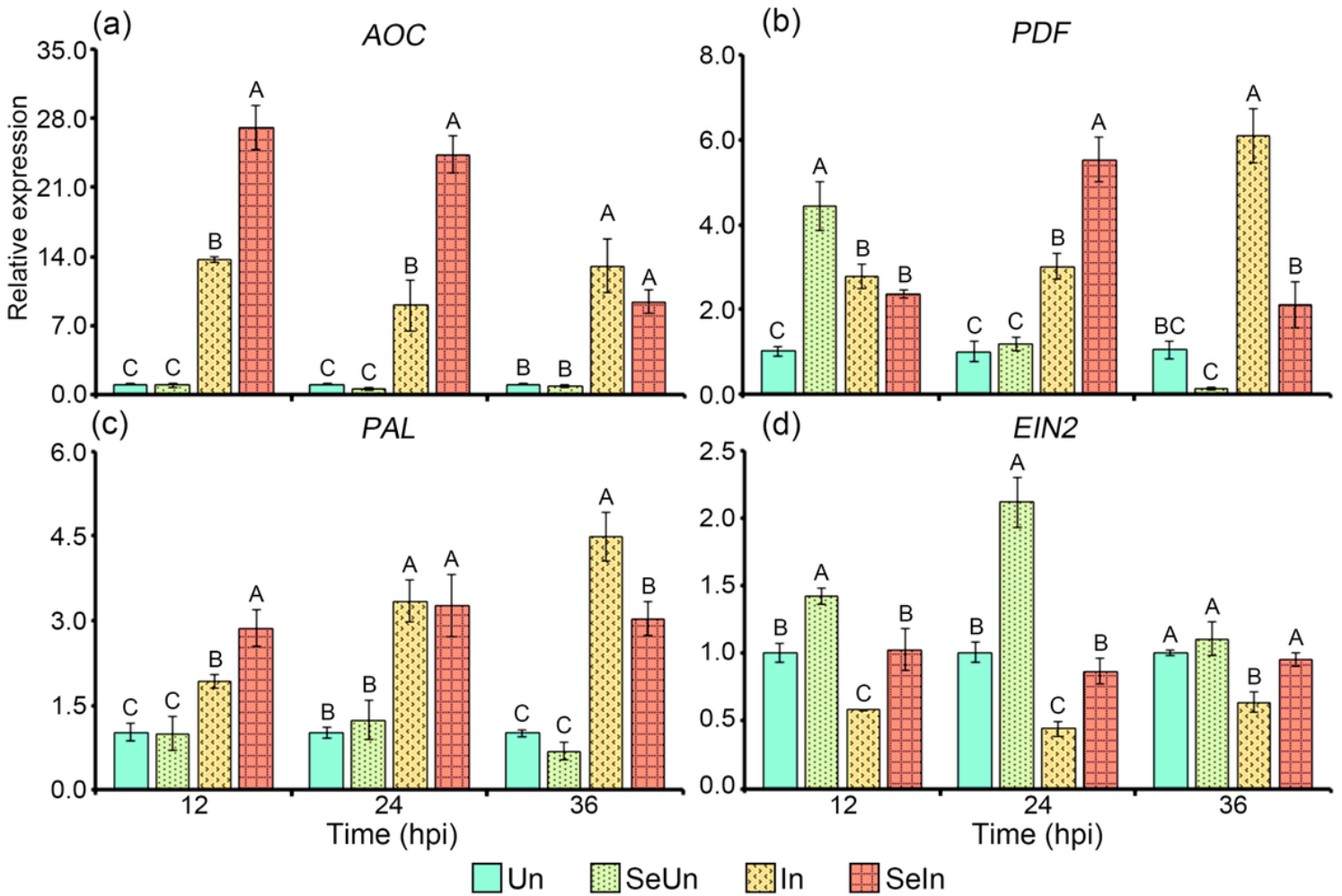


Figure 5

Evaluation of pathogen- or Se-mediated changes in transcript levels of critical genes involved in plant hormone signaling pathways. Data is shown as mean \pm standard error. Means in the plot topped by the same letter do not differ based on Duncan's multiple range test at $P < 0.05$ ($n = 3$).

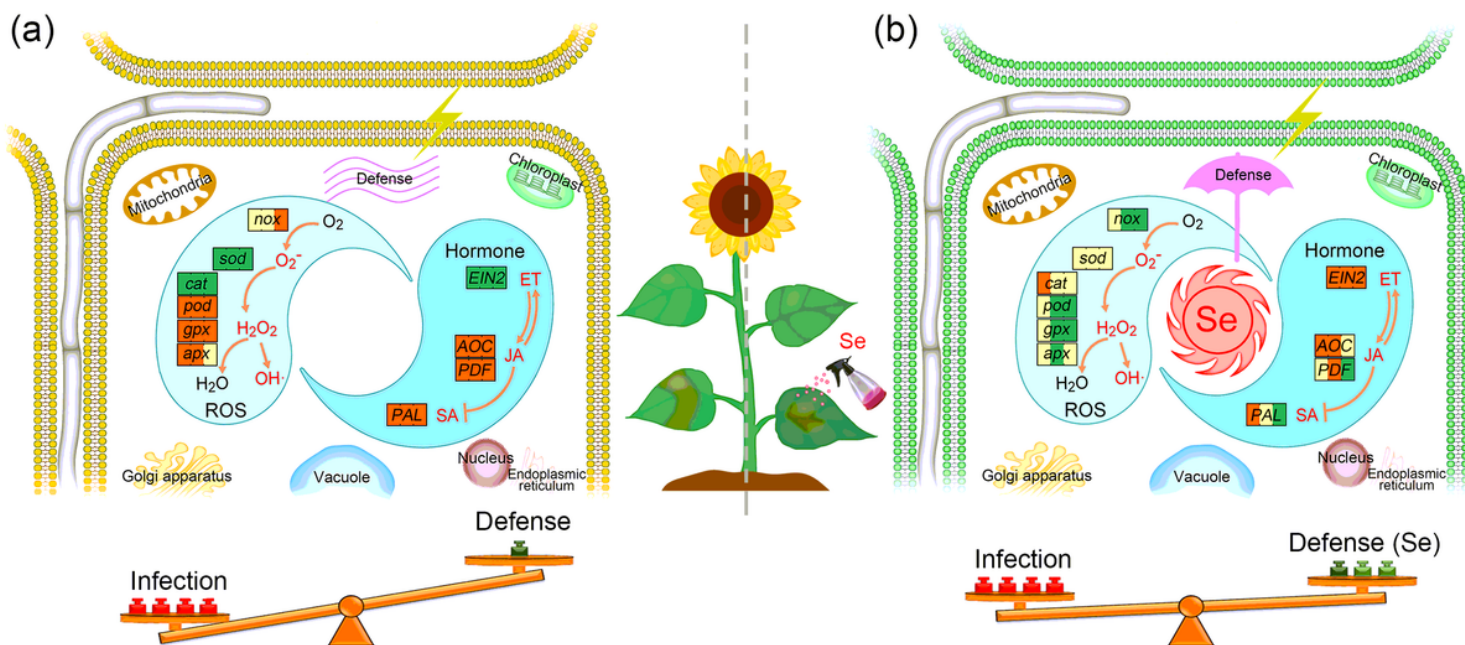


Figure 6

A model of pathogen- or Se-modulated changes in redox homeostasis and hormonal signaling pathways in sunflower challenged by *S. sclerotiorum*. The interplay of enzymes involved in redox homeostasis and hormonal signaling pathways were modeled for the In treatment compared with the Un treatment (a) and the SeIn treatment compared with In treatment (b), in which the relative expressions were indicated with the significant upregulation (red) and downregulation (green) during the infection.

Supplementary Files

This is a list of supplementary files associated with this preprint. Click to download.

- [SupplementaryInformation.docx](#)